Fermilab

CHARM AND BEAUTY PRODUCTION AND POLARIZATION AT CDF

Vaia Papadimitriou

Texas Tech University, Lubbock, TX 79409, U.S.A

Abstract

In this paper we present results on Charm and Beauty production as well as on production and polarization of Quarkonia at $\sqrt{s} = 1.8$ TeV. These results were obtained from data taken with the CDF detector at Fermilab. We cover recently completed analyses of the 1992-96 collider run.

1 Introduction

Charm, Beauty and heavy Quarkonia states, $c\bar{c}$ and $b\bar{b}$, provide very useful systems for the study of both perturbative and non perturbative QCD. The large production of such states in $p\bar{p}$ colliders and the ability to trigger on them efficiently make the Tevatron a unique place for such studies allowing the disentagling of various production mechanisms.

From August 1992 to February 1996, the CDF detector collected a data sample of 110 pb^{-1} of $p\bar{p}$ collisions at $\sqrt{s} = 1.8$ TeV and we refer to this period as Run I. We refer to the period from 1992-93 (~ 20 pb^{-1}) as Run Ia and to the period from 1994-1996 (~ 90 pb^{-1}) as Run Ib. The CDF detector is described in detail elsewhere [1], [2]. Here we describe some features of the detector, most relevant to the analyses we discuss. CDF has good tracking and lepton ID for the pseudorapidity region $|\eta| < 1$. The tracking system gives a transverse momentum resolution $\delta p_T/p_T = [(0.0009 \times p_T)^2 + (0.0066)^2]^{1/2}$, where p_T is in units of GeV/c. The average track impact parameter resolution relative to the beam axis is $(13 + (40/p_T))$ μm in the plane transverse to the beam, for $|z| < 25$ cm, the area covered by the Silicon Vertex detector (SVX). Muon candidates consist of tracks in the central tracking chamber matched to hits in muon chambers, located outside the calorimeter. Photon candidates consist of an energy deposit in the central electromagnetic calorimeter, matched to clusters in strip chambers embedded in the calorimeter.

This paper is organized as follows. In section 2 we describe results on Charm and Beauty production, in section 3 we describe results on Quarkonia production and their polarization and in section 4 we present conclusions and discuss the future prospects.

2 Charm and Beauty Production

2.1 Charm Production

Here we describe the first measurement of the $D^{*+}(2010)$ meson production cross section at the Tevatron. This measurement can probe into the charm-quark production which has not been measured in hadronic collisions so far. For this analysis we use the inclusive muon triggers from the Run Ib data set. We reconstruct D^{*+} events via the decay chain $D^{*+} \rightarrow D^0\pi_s^+$, $D^0 \rightarrow K\mu + X$, where π_s stands for "slow pion". We identify D^{*+} by using the mass difference $\Delta M =$M(K,μ,π_s^+)-M(K,μ). For the signal events or "Right Sign (RS)" events, the charge of the π_s is the same as that of the μ. The "Wrong Sign (WS)" events are defined as the ones for which the charge

of the π_s is opposite from the one of the μ. All tracks in this analysis are required to be reconstructed in the SVX and their minimum transverse momentum, p_T, is required to be 8 GeV/c for muons, 1 GeV/c for Kaons and 0.4 GeV/c for the slow pions. The π_s is also required to come from the primary interaction point. In fig. 1 we show the ΔM distribution. A requirement of $\Delta M < 0.18$ GeV/c^2 keeps high efficiency for the D^{*+} events and eliminates a large amount of background events. We require as well that the mass of $K\mu$ is in the range $0.9 < M_{K\mu} < 1.85$ GeV/c^2.
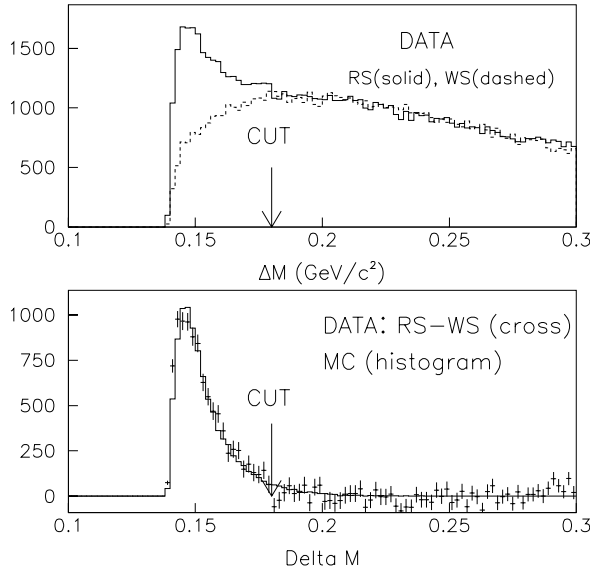

Figure 1: *The M(K,μ,π_s^+)-M(K,μ) distribution. In the top plot, we show both the Right Sign (RS) and the Wrong Sign (WS) events. The arrow shows the cut at 0.18 GeV/c^2. In the bottom plot, we show the distribution RS-WS (cross) and the Monte Carlo expectation (histogram).*

We observe 8,020$\pm$176 D^{*+} over 11,437 background events. The observed $D^{*\pm}$ events originate from both charm and bottom quarks. Since we reconstruct the D^0 decay vertex of the μ and the K with the SVX detector, we measure the fraction of the D^{*+} events from charm and bottom quarks by measuring the lifetime distribution of the D^0 events. From a fit between data and Monte Carlo histograms we find that the fraction of the D^{*+} events from bottom quarks is 2.1$\pm$2.1%, and therefore the measurement of the D^{*+} cross section is directly probing the charm quark cross section. In fig. 2 we show the differential D^{*+} production cross section. The crosses represent the data. The dashed curve is based on predictions by M.

Cacciari, M. Greco and P. Nason [3]. It is a next-to-leading order (NLO) calculation and it includes resummation of logs of p_T/m with NLL accuracy to all orders. This calculation uses CTEQ4M structure functions and a Peterson fragmentation parameter value of $\epsilon_P = 0.02$. The dotted curve is based on a prediction by M. Mangano [4] and it represents a fixed NLO calculation with $\epsilon_P = 0.078$. We observe a steeper falling transverse momentum spectrum of the differential cross section than the theoretical predictions. We measure the integrated D^{*+} cross section to be $347 \pm 65(\text{stat}) \pm 58(\text{sys})$nb for the kinematic range $|\eta(D^{*+})| < 1.0$ and $p_T(D^{*+}) > 10$ GeV/c. The measurement is higher than the theoretical prediction [3] of 240 nb, but consistent with it.
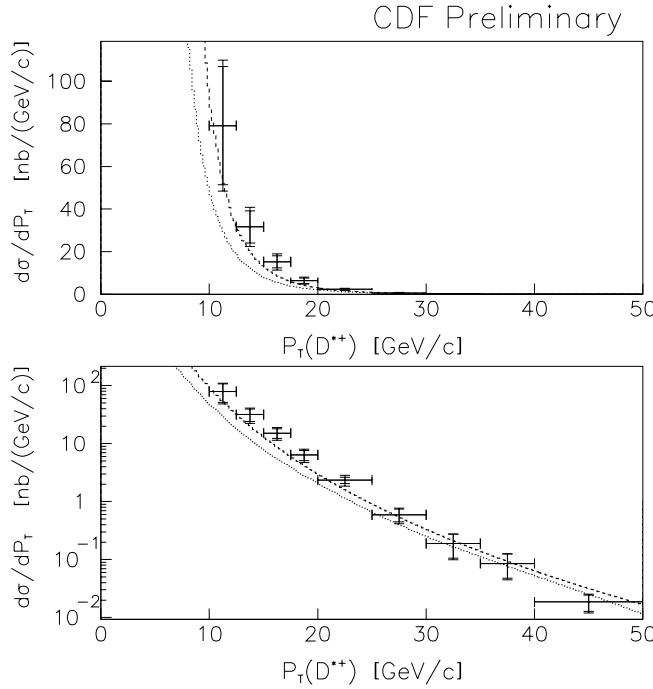

Figure 2: *The differential cross section of D^{*+} production in linear and logarithmic scales. The crosses represent the data. The inner error bars show the statistical error and the outer error bars represent the sum of the statistical and the systematic errors. The dashed and dotted curves represent theoretical predictions.*

2.2 Beauty Production

The exclusive decay $B^+ \to J/\psi K^+$; $J/\psi \to \mu^+\mu^-$ is used to measure the production cross section of the B^+ meson. The sample selection begins from data collected by

the dimuon trigger. Both muon tracks are required to be reconstructed in the SVX detector to improve vertex resolution. The Kaon and the B meson are required to have p_T greater than 1.25 GeV/c and 6.0 GeV/c respectively. A sample size of 387±32 $B^\pm$ events is obtained from 104.7±4.3 pb^{-1} of data. In fig. 3 we show the differential cross section compared with the NLO QCD calculation by Nason-Dawson-Ellis (NDE) [5]) using the MRST structure functions. The dashed lines indicate the change in the theoretical predictions as the b quark mass is varied between 4.5 and 5.0 GeV/c^2, the renormalization scale is varied between $\mu_0/2$ and $2\mu_0$, and the Peterson fragmentation parameter is varied between 0.004 and 0.008. The solid curve is for the central values of these parameters: $m_b = 4.75$ GeV/c^2, $\mu_0 = \sqrt{m_b^2 + p_T^2}$, and $\epsilon_P = 0.006$. The shape of the B^+ meson differential cross section is adequately described by NLO QCD. The measured total B^+ production cross section for $p_T(B^+) > 6.0$ GeV/c and rapidity range $|y(B)| < 1$ is 3.51±0.42(stat)±0.53(sys) μb. The corresponding value of the theoretical cross section [5]) is 1.54 μb.

B$^+$ Meson Differential Cross Section

CDF Preliminary

— NLO QCD: MRST, $\mu_0 = \sqrt{(m_b^2 + p_T^2)}$
$m_b = 4.75$ GeV/c^2, $\epsilon_P = 0.006$, $f_u = 0.375$
······ Theoretical Uncertainty

Systematic + Statistical Error
Statistical Error

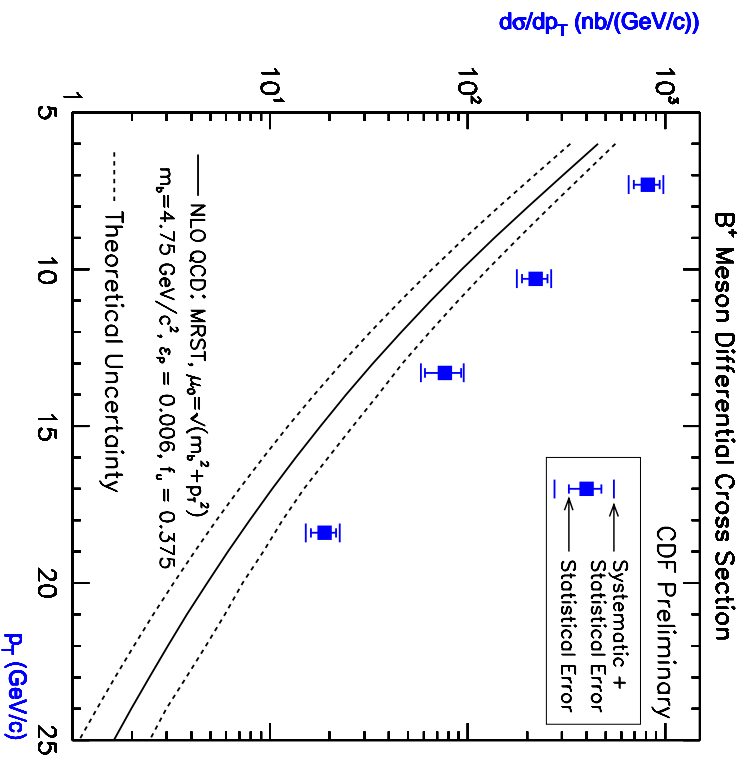dσ/dp$_T$ (nb/(GeV/c))

p$_T$ (GeV/c)

Figure 3: *B^+ meson differential cross section measurement compared to the theoretical prediction.*

3 Quarkonia Production and Polarization

3.1 J/ψ and $\psi(2S)$

The CDF collaboration has previously reported results on the production of J/ψ and $\psi(2S)$ mesons [6], [7]. The measured cross sections for direct production were on the order of 50 times larger than predicted by the Color Singlet Model(CSM) [8]. However, calculations based on the Nonrelativistic QCD (NRQCD) factorization formalism [9] are able to account for the observed cross sections by including color octet production mechanisms. This leads to the prediction that directly produced ψ mesons will be increasingly transversely polarized at high p_T [10], [11], [12]. (In this paper we use ψ to denote either J/ψ or $\psi(2S)$ mesons.) This is because the production of ψ mesons with $p_T >> M_\psi$ is dominated by gluon fragmentation and it is predicted that the gluon's transverse polarization is preserved as the $c\bar{c}$ pair evolves into a bound state ψ meson. On the other hand the Color Evaporation Model predicts an absence of polarization [13]. The data used in this study correspond to ~ 110 pb^{-1} and were collected with the dimuon trigger. The measurement of the polarization of J/ψ and $\psi(2S)$ mesons is made by analyzing their decays to $\mu^+\mu^-$ in the helicity basis, in which the spin quantization axis lies along the ψ direction in the $p\bar{p}$ center-of-mass frame. The angle θ is given by the direction of the μ^+ in the ψ rest frame and the ψ direction in the $p\bar{p}$ center-of-mass frame. The normalized angular distribution $I(\theta)$ is given by $I(\theta) = \frac{3\cdot(1+\alpha cos^2\theta)}{2(\alpha+3)}$. Unpolarized ψ mesons have $\alpha = 0$ while $\alpha = +1$ or -1 correspond to fully transverse or longitudinal polarizations respectively.

Our method of determining α is to fit the observed distributions of $cos\theta$ to distributions derived from simulated $\psi \to \mu^+\mu^-$ decays. In order to extract the polarization parameter α for promptly produced ψ mesons, we separate the prompt component (α_P) from the B-decay component (α_B) using the proper decay length of each event. The J/ψ polarization is measured in seven p_T bins covering the range 4-20 GeV/c. In fig. 4 we show our fit results for α_P and α_B and we compare α_P with a theoretical NRQCD prediction [12]. The measurement of the $\psi(2S)$ polarization is measured in three p_T bins covering the region 5.5-20.0 GeV/c. The fitted values for α_P and α_B as a function of $P_T^{\psi(2S)}$ are shown in fig. 5 together with two NRQCD predictions. The polarization from B decays (α_B) is generally consistent with zero, as expected. In both the J/ψ and $\psi(2S)$ states, we do not observe increasing prompt transverse polarization for $p_T \geq 12$ GeV/c, in disagreement with NRQCD factorization predictions [11], [12].
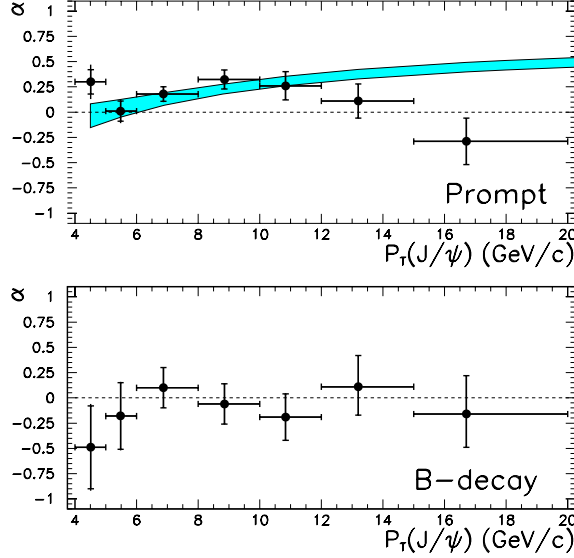
Figure 4: *The fitted polarization of J/ψ mesons from prompt production and B-hadron decay, in seven p_T bins, for $|y^{J/\psi}| < 0.6$. The shaded band shows an NRQCD factorization prediction [12] which includes the contribution from χ_c and $\psi(2S)$ decays.*

3.2 χ_c

Using ~ 18 pb^{-1} of data from Run Ia we studied [7] the reaction $p\bar{p} \to \chi_c X$; $\chi_c \to J/\psi\gamma$ and have identified 1230 ± 72 χ_c signal events. For $p_T(J/\psi) > 4.0$ GeV/c and $|\eta(J/\psi)| < 0.6$ we have measured the fraction of J/ψ mesons originating from χ_c meson decays to be $29.7\pm1.7(\text{stat})\pm5.7(\text{sys})\%$, not including contributions from b hadrons. This fraction is approximately independent of $p_T^{J/\psi}$ between 4 and 15 GeV/c. We have also found that the fraction of prompt J/ψ's from $\psi(2S)$'s rises from $7\pm2\%$ at $p_T^{J/\psi} = 5$ GeV/c to $15\pm5\%$ at $p_T^{J/\psi} = 18$ GeV/c. The fraction of directly produced J/ψ's is $64\pm6\%$ and it is approximately independent of $p_T^{J/\psi}$ between 5 and 18 GeV/c. Direct production is therefore the largest source of prompt J/ψ mesons. We used the above fraction measurements to subtract from the prompt J/ψ cross section the contribution from χ_c and $\psi(2S)$ decays and derive the direct J/ψ differential cross section discussed in the previous section. Using ~ 110 pb^{-1} of data, we have also measured the relative rate of production of the charmonium states χ_{c1} and χ_{c2} through their decay into $J/\psi\gamma$. The photon from the decay is reconstructed here through conversion into e^+e^- pairs, which makes the resolution of the two states possible. The effective lifetime (λ_{eff}) is used to discriminate between
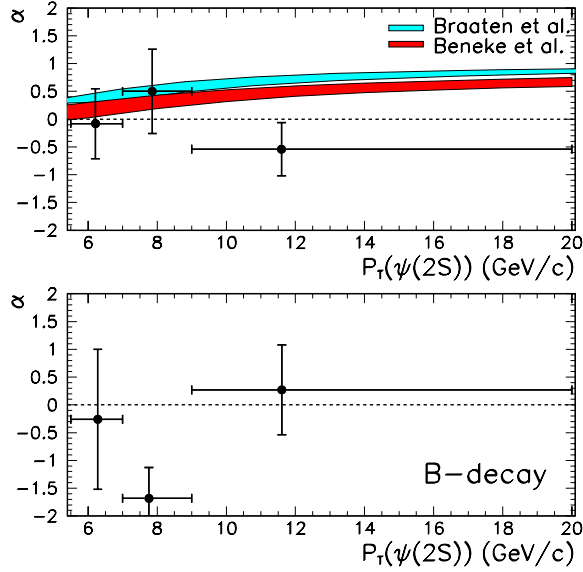
Figure 5: *The fitted polarization of $\psi(2S)$ mesons from prompt production and B-hadron decay, in three p_T bins, for $|y^{\psi(2S)}| < 0.6$. The prompt polarization is compared with two NRQCD factorization predictions* [11], [12].

χ_c events produced promptly and through B decay processes. The predominant χ_{cJ} background is believed to be due to photons resulting from the decay of π^0, η and K_s^0 produced in association with the J/ψ. Although the existence of the process is poorly established, we nonetheless consider a second source of background due to the partial reconstruction of $h_c(1P) \to J/\psi \pi^0; \pi^0 \to \gamma\gamma$. The $J/\psi\gamma$ mass spectrum for $\lambda_{eff} < 100\mu m$ is shown in fig. 6. The χ_{c1} and χ_{c2} signals are determined by performing a least squares fit on the $J/\psi\gamma$ mass spectrum with a function that contains two gaussians and a background shape determined by Monte Carlo calculation. Two versions of this fit are performed, one where the $h_c(1P)$ component varies, and one where it is constrained to zero amplitude. We find 39.2 ± 8.3 and 21.3 ± 6.2 χ_{c1} and χ_{c2} events respectively assuming zero contribution from the $h_c(1P)$ state. We find the ratio of production cross sections $\frac{\sigma_{\chi_{c2}}}{\sigma_{\chi_{c1}}} = 0.89\pm0.33\text{(stat)} ^{+0.13}_{-0.10}\text{(sys)}$ for events with $p_T(J/\psi) > 4.0$ GeV/c, $|\eta(J/\psi)| < 0.6$ and $p_T(\gamma) > 1.0$ GeV/c. The systematic uncertainty here includes the contribution of the $h_c(1P) \to J/\psi\pi^0$ in the event yield ratio. A recent NRQCD prediction [14] for the cross section ratio is equal to 1.1 ± 0.2, in good agreement with this measurement.

3.3 Υ's and χ_b's

Using ~ 77 pb^{-1} of dimuon trigger data from Run Ib we identify 4430 ± 95 Υ(1S) events, 1114 ± 65 Υ(2S) events and 584 ± 53 Υ(3S) events in the rapidity region $|y(\Upsilon)| <0.4$ and for 0 GeV/c $< p_T(\Upsilon) < 20$ GeV/c. The Υ mass distributions are then fitted as a function of the dimuon p_T in order to extract differential cross sections. These cross sections are higher than CSM predictions [15] by factors between 3-5 for $p_T^{\Upsilon} >3$ GeV/c. The p_T shape cannot be reproduced by CSM in the $p_T^{\Upsilon} <3$ GeV/c region.

Using ~ 90 pb^{-1} of data from Run Ib we have also searched for the radiative decays of χ_b and see evidence for $\chi_b(1P) \rightarrow \Upsilon(1S)\gamma$ and $\chi_b(2P) \rightarrow \Upsilon(1S)\gamma$ for relatively high $p_T^{\Upsilon(1S)}$. Υ(1S) candidates with $p_T > 8$ GeV/c (1462 ± 55 events) are combined with photon candidates with energy greater than 0.7 GeV. We show the $\Delta M = M(\mu^+\mu^-\gamma) - M(\mu^+\mu^-)$ mass distribution in fig. 7. The number of χ_b signal events is determined by fitting the data ΔM distribution to the sum of the background distribution and two gaussian functions associated with the signals. The fit results in 35.3 ± 9.0 and 28.5 ± 12.0 signal events for $\chi_b(1P)$ and $\chi_b(2P)$ respectively. We have measured the fractions of Υ(1S) mesons originating from $\chi_b(1P)$, $\chi_b(2P)$ and $\chi_b(3P)$ decays to be 27.1 ± 6.9(stat)±4.4(sys)%, 10.5 ± 4.4(stat)±1.4(sys)% and less than 6% respectively for $p_T^{\Upsilon(1S)} > 8$ GeV/c. For the same kinematic region we have also found that the fractions of Υ(1S) mesons originating from Υ(2S) and Υ(3S) mesons are $10.7^{+7.7}_{-4.8}$% and $0.8^{+0.6}_{-0.4}$% respectively. The fraction of directly produced Υ(1S) mesons was measured to be 50.9 ± 8.2(stat)±9.0(sys)%.

We have also performed a polarization analysis on the Υ(1S) data sample in a similar way to that on the ψ sample. We study again the angle θ given by the direction of the μ^+ in the Υ(1S) rest frame and the Υ direction in the $p\bar{p}$ center-of-mass frame. Here we do not have the complication of having to separate the prompt decays from the B decays. In the range $2 < p_T < 20$ GeV/c the fitted longitudinal fraction is $\Gamma_L/\Gamma = 0.37 \pm 0.04$, corresponding to an α of -0.08 ± 0.09, consistent with unpolarized Υ's. In the more restricted range $8 < p_T < 20$ GeV/c the fitted fraction is $\Gamma_L/\Gamma = 0.32 \pm 0.11$ corresponding to an α of 0.03 ± 0.25, again consistent with unpolarized Υ's. This result does not contradict predictions including color octet mechanisms since transverse polarization is expected to be large only for $p_T >> M_\Upsilon$.

4 Conclusions-Prospects

In this paper we have presented results on Charm, Beauty and Quarkonia production as well as on Quarkonia Polarization. The Charm, Beauty and Quarkonia cross

sections are higher than the theoretical expectations. The polarization of the J/ψ and $\psi(2S)$ mesons does not increase as a function of the ψ p_T, in disagreement with NRQCD factorization predictions. We have measured the fractions of J/ψ originating from other charmonia states or produced directly and the fractions of $\Upsilon(1S)$ produced from other botommonia states or produced directly. We measured the ratio of χ_{c2} over χ_{c1} cross sections to be consistent with NRQCD theoretical expectations.

The Tevatron will commence $p\bar{p}$ collisions again at $\sqrt{s} = 2.0$ TeV in March of 2001 with an initial goal of delivering an integrated luminosity of 1 fb^{-1} per year, corresponding to approximately 10^{11} $b\bar{b}$ pairs produced per year. This upcoming data taking period is referred to as Run II. We expect to collect a data sample of more than 15 fb^{-1} before 2007 which will allow us to further investigate and shed more light on the Charm, Beauty and Quarkonia production and polarization mechanisms.

5 Acknowledgements

References

1. F. Abe *et al.*, Nucl. Instrum. Methods A**271** 387 (1988).

2. F. Abe *et al.*, Phys. Rev. D**50**, 2966 (1994).

3. M. Cacciari, M. Greco, P. Nason, J. High Energy Phys. 05, 007 (1998); M. Cacciari, M. Greco, Phys. Rev. D**55**, 7134 (1997).

4. M. Mangano *et al*, Nucl. Phys. B**373**, 295 (1992).

5. P. Nason *et al*, Nucl. Phys. B**327**, 49 (1989); P. Nason *et al*, Nucl. Phys. B**335**, 260 (1990).

6. F. Abe *et al.*, Phys. Rev. Lett.**79**, 572 (1997).

7. F. Abe *et al.*, Phys. Rev. Lett.**79**, 578 (1997).

8. M. Cacciari, M. Greco, Phys. Rev. Lett.**73**, 1586 (1994); E. Braaten *et al.*, Phys. Lett.B**333**, 548 (1994); D.P. Roy and K. Sridhar, Phys. Lett.B**339**, 141 (1994).

9. G. Bodwin, E. Braaten and G. Lepage, Phys. Rev. D**51**, 1125 (1995) (Erratum *ibid.* **55**, 5853 (1997)); E. Braaten and S. Fleming, Phys. Rev. Lett.**74**, 3327 (1995); M. Cacciari *et al*, Phys. Lett.B**356**, 553 (1995); E. Braaten and Y. Chen, Phys. Rev. D**54**, 3216 (1996); P. Cho and A.K. Leibovich, Phys. Rev. D**53**, 150, (1996), P. Cho and A.K. Leibovich, Phys. Rev. D**53**, 6203 (1996).

10. P. Cho and M. Wise, Phys. Lett.B**346**, 129 (1995).

11. M. Beneke and M. Kramer, Phys. Rev. D**55**, 5269 (1997).

12. E. Braaten, B. Kniehl and J. Lee, hep-ph/9911436.

13. J. Amundson *et al.*, Phys. Lett.B**390**, 323 (1997).

14. F. Maltoni, private communication. Work based on [9].
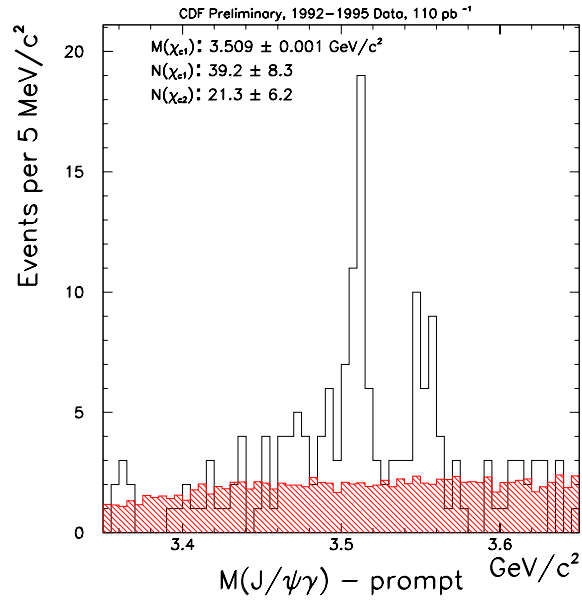
15. A. Leibovich, private communication. Work based on [8].

Figure 6: *The J/ψγ mass spectrum. The solid line histogram shows the data. The background estimate due to prompt sources is indicated by the shaded area.*
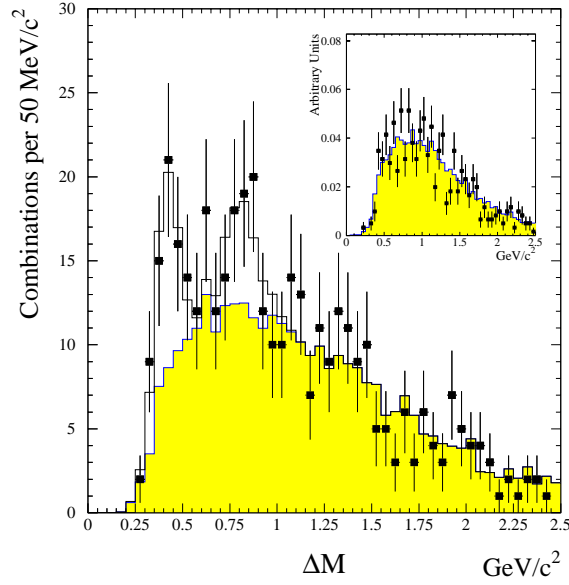
Figure 7: *The* $\Delta M = M(\mu^+ \mu^- \gamma) - M(\mu^+ \mu^-)$ *distribution. The points represent the data. The shaded histogram is the background shape predicted by the Monte Carlo calculation. The solid line is the fit of the data to two gaussian functions plus the background histogram. The inset shows the comparison between the* ΔM *distribution for dimuons in the* $\Upsilon(1S)$ *sidebands and the corresponding one predicted by the Monte Carlo calculation.*